

Alma Mater Studiorum Università di Bologna  
Archivio istituzionale della ricerca

The follicle-sinus complex of the bottlenose dolphin (*Tursiops truncatus*). Functional anatomy and possible evolutionary significance of its somato-sensory innervation

This is the final peer-reviewed author's accepted manuscript (postprint) of the following publication:

*Published Version:*

Gerussi, T., Graic, J.-., De Vreese, S., Grandis, A., Tagliavia, C., De Silva, M., et al. (2021). The follicle-sinus complex of the bottlenose dolphin (*Tursiops truncatus*). Functional anatomy and possible evolutionary significance of its somato-sensory innervation. JOURNAL OF ANATOMY, 238(4), 942-955 [10.1111/joa.13345].

*Availability:*

This version is available at: <https://hdl.handle.net/11585/835475> since: 2021-10-19

*Published:*

DOI: <http://doi.org/10.1111/joa.13345>

*Terms of use:*

Some rights reserved. The terms and conditions for the reuse of this version of the manuscript are specified in the publishing policy. For all terms of use and more information see the publisher's website.

This item was downloaded from IRIS Università di Bologna (<https://cris.unibo.it/>).  
When citing, please refer to the published version.

(Article begins on next page)

THE FOLLICLE-SINUS COMPLEX OF THE BOTTLENOSE DOLPHIN (*Tursiops truncatus*). FUNCTIONAL ANATOMY AND POSSIBLE EVOLUTIONAL SIGNIFICANCE OF ITS SOMATO-SENSORY INNERVATION.

**Authors:**

Tommaso Gerussi<sup>1</sup>; Jean-Marie Graïc<sup>1</sup>; Steffen de Vreese<sup>1,4</sup>; Annamaria Grandis<sup>2</sup>; Claudio Tagliavia<sup>2</sup>; Margherita De Silva<sup>2</sup>; Stefan Huggenberger<sup>3</sup>, Bruno Cozzi<sup>1</sup>.

**Affiliations:**

<sup>1</sup>Department of Comparative Biomedicine and Food Science (BCA) University of Padua, Viale dell'Università 16, 35020, Legnaro (PD), Italy

<sup>2</sup>Department of Veterinary Medical Sciences, University of Bologna, Via Tolara di Sopra 50, 40064, Ozzano dell'Emilia (BO), Italy

<sup>3</sup> Institute of Anatomy and Clinical Morphology, Faculty of Health, Witten/Herdecke University, Alfred-Herrhausen-Straße 50, 58448 Witten, Germany

<sup>4</sup>Laboratory of Applied Bioacoustics (LAB), Technical University of Catalonia, Barcelona Tech (UPC), Puerto pesquero s/n, 08800 Vilanova i la Geltru, Spain

Gerussi: 0000-0003-0263-5635

Graïc: 0000-0002-1974-8356

De Vreese: 0000-0001-5007-5850

Grandis: 0000-0003-0292-5261

Tagliavia: 0000-0002-8628-693X

De Silva: 0000-0003-0627-4427

Huggenberger: 0000-0002-8085-5927

Cozzi: 0000-0002-7531-7040

**Corresponding author:**

Jean-Marie Graïc

ORCID: 0000-0002-1974-8356

Department of Comparative Biomedicine and Food Science (BCA)

University of Padua,

Viale dell'Università 16,

35020, Legnaro (PD), Italy

Tel: +39 049 827 2547

Email: jeanmarie.graic@unipd.it

## Abstract

Vibrissae are tactile hairs found mainly on the rostrum of most mammals. The follicle which is surrounded by a large venous sinus is called "follicle sinus complex" (FSC). This complex is highly innervated by somatosensitive fibers and reached by visceromotor fibers that innervate the surrounding vessels. The surrounding striate muscles receive somatomotor fibers from the facial nerve. The bottlenose dolphin (*Tursiops truncatus*), a frequently described member of the delphinid family, possesses this organ only in the postnatal period. However, information on the function of the vibrissal complex in this latter species is scarce. Recently, psychophysical experiments on the river-living Guiana dolphin (*Sotalia guianensis*) revealed that the FSC could work as an electroreceptor in murky waters. In the present study we analyzed the morphology and innervation of the FSC of newborn (n. = 8) and adult (n. = 3) bottlenose dolphins. We used Masson's trichrome stain and antibodies against neurofilament 200 kDa (NF 200), protein gene product (PGP 9.5), substance P (SP), calcitonin gene related peptide (CGRP) and tyrosine hydroxylase (TH) to characterize the FSC of the two age classes. Masson's trichrome staining revealed a structure almost identical to that of terrestrial mammals except for the fact that the FSC was occupied only by a venous sinus and that the vibrissal shaft lied within the follicle. Immunostaining for PGP 9.5 and NF 200 showed somatosensory fibers finishing high along the follicle with Merkel nerve endings and free nerve endings. We also found SP-positive fibers mostly in the surrounding blood vessels and TH both in the vessels and in the mesenchymal sheath. The FSC of the bottlenose dolphin, therefore, possesses a rich somatomotor innervation and a set of peptidergic visceromotor fibers. This anatomical disposition suggests a mechanoreceptor function in the newborns, possibly finalized to search for the opening of the mother's nipples. In the adult, however, this structure could change into a proprioceptive function in which the vibrissal shaft could provide information on the degree of rotation of the head. In the absence of psychophysical experiments in this species, the hypothesis of electroreception cannot be rejected.

(344 words)

## Keywords:

Vibrissae; Whiskers; Follicle-Sinus Complex; Innervation; *Tursiops truncatus*; bottlenose dolphin

## 31 **Introduction**

32 Vibrissae, also called whiskers, are modified tactile hairs that occur in most mammals except  
33 monotremes, anteaters, rhinoceroses, and humans (Cave, 1969; Van Horn, 1970; Chernova, 2006;  
34 Muchlinski, 2010). They are mainly located around the muzzle but can be also present in other parts  
35 of the head and under the carpus, depending on the species (Fundin *et al.*, 1995; Sarko *et al.*, 2011).  
36 Their main function is to convey mechanical (tactile) stimuli to the somatosensory cortex (Woolsey  
37 and Van der Loos, 1970). The hair follicle of each vibrissa is surrounded by a large venous sinus,  
38 together forming the “Follicle-Sinus Complex” (FSC) (Rice *et al.*, 1986). The presence of vibrissae  
39 in Pinnipeds, Odobenids, Sirenids and otters, suggests that their somatosensory function is functional  
40 also in the water. However, vibrissae are present only in newborn cetaceans and generally disappear  
41 in adults. Therefore the question arises if the vibrissae of very young cetaceans perform a temporary  
42 function that is lost within a few weeks after birth, or are just a remnant of a structure that evolution  
43 discarded in these mammals.

44  
45 The morphology and innervation of the vibrissae have been studied extensively in rodents and cats  
46 (Rice *et al.*, 1986, 1993; Ebara *et al.*, 2002; Park *et al.*, 2003), and thus our present knowledge of the  
47 structure and function of the FSC mostly derives from these species, although efforts have been  
48 developed in marsupials (Lyne, 1958; Hollis and Lyne; 1974; Marotte *et al.*, 1992). In general, the  
49 FSC of terrestrial mammals consists of epidermal and dermal components. The epidermal parts  
50 include the hair bulb, the vibrissal shaft (VS), the inner and outer root sheaths, surrounded by a glassy  
51 membrane. The latter separates these components from the dermal parts, that is the mesenchymal  
52 sheath (MS) and the venous sinus. The sinus is horizontally divided into a proximal ring sinus  
53 (containing the ringwulst and the inner conical body), and a distal cavernous sinus (that contains a  
54 large number of trabeculae, filled with venous blood). The last dermal part is the connective tissue  
55 capsule that limits the follicle and caps it above the inner conical body with the outer conical body.  
56 Finally, the rete ridge collar is a thickening of the epidermis where the VS protrudes (Rice *et al.*,  
57 1986, Ebara *et al.*, 2002).

58  
59 As mentioned above, marine mammals also develop vibrissae, and a description of their morphology  
60 and dimensions in seals and otter has been recently reported in comparison with several terrestrial  
61 species (Dougill *et al.*, 2020). Walruses have the highest number of vibrissae (up to 350 on each side),  
62 while pinnipeds possess large and richly innervated FSCs, divided in three parts, with up to 1600  
63 axons reaching it (Hyvärinen, 1989, 1995; Hyvärinen *et al.*, 2010; Ling, 1966, 1977; Marshall *et al.*,  
64 2006). In manatees, extensive studies have described the vibrissae, which are spread out on the

65 muzzle and the body (Reep *et al.*, 1998, 2001; Sarko *et al.*, 2007). Mysticetes have vibrissae in large  
66 quantity caudally to the blowhole and on the rostro-lateral sides of the upper and lower jaws with  
67 numbers up to 250 in the bowhead whale (*Balaena mysticetus*) (Slijper, 1962; Yablokov and  
68 Klevezal, 1964). On the contrary, most adult toothed whales have no facial hair and show 2-10  
69 bilateral rows of vibrissae only during fetal life and the early postnatal period (Yablokov *et al.*, 1972;  
70 Ling, 1977; Reidenberg and Laitman, 2009). Toothed whales show fully developed vibrissae only in  
71 the early phases of their post-natal life (Czech-Damal *et al.* 2013; Cozzi *et al.*, 2017; Dehnhardt and  
72 Hanke, 2017). From morphological comparisons among odontocetes, a classification divided them  
73 into four groups based on the development of the FSC (Yablokov *et al.*, 1972). Following this  
74 classification, the bottlenose dolphin falls into a group comprising species in which the VS is still  
75 present in the early postnatal period but disappears in the majority of adult individuals. This is not the  
76 case in river dolphins such as the Guiana dolphin (*Sotalia guianensis*) of which a recent study  
77 described the FSC (Czech-Damal *et al.*, 2012). The FSC of this species was renamed *vibrissal crypt*  
78 because of its different anatomical structure, characterized by the absence of the VS, hair papilla,  
79 clear root sheaths, blood sinus and capsule (Czech-Damal *et al.*, 2012). The FSC lumen is filled with  
80 desquamated corneocytes and keratinous fibers, that together may be considered a highly electrically  
81 conductive biogel (Czech-Damal *et al.*, 2012), part of an electrosensory system that facilitates the  
82 hunt of small bottom-living prey in turbid water, where echolocation is not possible or potentially not  
83 efficient enough, by detection of their electric field (Czech-Damal *et al.*, 2012).

84 The somatosensory innervation of mystacial vibrissae is provided by three subdivisions of the  
85 maxillary branch of the trigeminal nerve. The deep vibrissal nerve, originates directly from the  
86 infraorbital nerve, supplies a single FSC, penetrates the capsule and arborizes dorsally at various  
87 levels. The superficial vibrissal nerves (SVNs) come from superficial cutaneous nerves and supply  
88 several FSCs. Small- to fine-caliber nerve fiber branches reach the FSC from the base and supply the  
89 hair papilla and hair bulb (Rice *et al.*, 1986; Ebara *et al.*, 2002). The deep vibrissal nerve ends in  
90 mechanoreceptors such as Merkel nerve endings (MNEs), lanceolate endings and free nerve endings  
91 (FNEs) along the follicle. The SVNs, instead, provide innervation to lanceolate endings at the level  
92 of inner conical body and MNEs at the level of the rete ridge collar (Fundin *et al.*, 1997a; Ebara *et al.*,  
93 2002). The somatomotor innervation is provided by motoneurons placed in the lateral part of the  
94 facial nucleus and innervates the extrinsic (mimic) and intrinsic musculature of the mystacial pad  
95 (Haidarliu *et al.*, 2010; Herfst and Brecht, 2008). The visceral innervation (sympathetic and  
96 parasympathetic) regulates blood flow in the FSC, supplied by the deep vibrissal artery, and  
97 consequently regulates blood pressure, which is essential for the activation of receptors that respond  
98 to specific stimulation thresholds. (Fundin *et al.*, 1997b, Maklad *et al.*, 2004).

99 Here we describe the FSC in a series of postnatal and adult bottlenose dolphins, aiming at  
100 characterizing the changes in the anatomy and morphology of this structure at different life stages by  
101 histochemical and immunohistochemical techniques. Special attention was dedicated to the  
102 innervation of the FSC, the nature of the nerve fibers, and its functional potential.

103

## 104 **Material and methods**

105

### 106 a) Animals

107 The samples of vibrissae from 11 bottlenose dolphins (*Tursiops truncatus*, Montagu 1821) were  
108 obtained from the Mediterranean Marine Mammal Tissue Bank (MMMTB,  
109 <http://www.marinemammals.eu>), housed in the Department of Comparative Biomedicine and Food  
110 Science (BCA) of the University of Padova. The MMMTB is a CITES recognized institution (IT 020)  
111 that collaborates with the Italian Ministry of the Environment. The MMMTB collects, processes, and  
112 stores samples of tissues of various cetacean species that stranded along the Italian coastline since  
113 2000. Additional samples derived from marine mammals that died at marine theme parks and aquaria,  
114 and whose bodies were delivered to BCA for diagnostic post-mortem. More details of the specimens  
115 used in this study can be seen in Table 1.

### 116 b) Sample processing

117 Each sample was obtained by carving out around the VS on both sides of the rostrum in the newborn  
118 and around the dimple containing the orifice in the adult (Figure 1a, b).  
119 The samples were fixed by immersion in 4% neutral buffered paraformaldehyde and stored at 4 °C.  
120 Tissues for Masson's trichrome were then included in paraffin and cut in 5 µm- and 10 µm-thick  
121 sections either longitudinal or transversal to the main axis of the FSC by use of a rotatory microtome  
122 (Leica, Germany). Sections were mounted on gelatinized slides and air dried. Samples bound for  
123 immunocytochemistry were washed in standard phosphate buffer solution (PBS) overnight at 4 °C,  
124 stored in PBS containing 0.1% Na-azide and sucrose at 30%, immersed in OCT Compound (Tissue  
125 Tek, Sakura Finetek Europe, NL) and frozen at -80 °C in isopentane cooled with liquid nitrogen. 25  
126 µm-thick sections of the longitudinal and transversal planes were subsequently taken with a cryostat  
127 (Leica, Germany).

128 **Table 1:** Origin of specimens

| ID    | Species             | Sex | Age class | Origin                      |
|-------|---------------------|-----|-----------|-----------------------------|
| # 83  | <i>T. truncatus</i> | M   | Newborn   | Died in a marine theme park |
| # 114 | <i>T. truncatus</i> | M   | Newborn   | Died in a marine theme park |
| # 123 | <i>T. truncatus</i> | F   | Newborn   | Died in a marine theme park |
| # 124 | <i>T. truncatus</i> | M   | Newborn   | Died in a marine theme park |
| # 144 | <i>T. truncatus</i> | M   | Newborn   | Died in a marine theme park |
| # 145 | <i>T. truncatus</i> | M   | Newborn   | Died in a marine theme park |
| # 162 | <i>T. truncatus</i> | M   | Newborn   | Wild                        |

|       |                     |   |         |                             |
|-------|---------------------|---|---------|-----------------------------|
| # 229 | <i>T. truncatus</i> | M | Newborn | Died in a marine theme park |
| # 146 | <i>T. truncatus</i> | M | Adult   | Died in a marine theme park |
| # 159 | <i>T. truncatus</i> | M | Adult   | Died in a marine theme park |
| # 444 | <i>T. truncatus</i> | M | Adult   | Wild                        |

c) Histological techniques:

The morphology of the FSC was stained using a Masson's trichrome staining protocol. Briefly, the sections were immersed in 3 baths of xylene for 5 minutes each and subsequently hydrated with a descending series of graded alcohol solutions (100 %, 95 %, 90 %, 80 %, 70 %, 50 %). Then, they were stained with Mayer's Emallume for 5-10 minutes and rinsed with tap water. Later, the sections were colored for 5 minutes in a solution of distilled water (300 ml) containing Ponceau 2R (0,2 g), acid fuchsin (0,1 g) and acetic acid (0,6 ml). After rinsing with a 1% acetic acid solution, the sections were put in a solution of distilled water (100 ml), phosphomolybdic acid (3-5 g) and orange G (2 g), for 5 minutes, and rinsed again in an acetic acid solution. The sections were then colored for 5 minutes in light green (0,1-0,2 g in 100 ml distilled water) and acetic acid (0,2 ml). After the last rinsing in a 1% acetic acid solution, the slides were dehydrated directly with absolute alcohol, and passed in xylene (3 x 3 minutes) and coverslipped with Entellan (Merck, Darmstadt, Germany).

The innervation of the FSC was characterized with immunocytochemistry, either *via* immunoperoxidase (IP) or immunofluorescence (IF), using the neuronal markers shown in Table 2. For IP staining, contiguous sections were initially immersed in a 0,4% solution of Triton X-100 (Merck, Darmstadt, Germany) in PBS at 4 °C for 24 hours. They were then rinsed in PBS baths for 3 x 10 minutes. Next, sections were treated with 1% H<sub>2</sub>O<sub>2</sub> in PBS for 30 minutes. After three 10-minute washes in PBS, a 3% solution of normal goat serum (NGS, Sigma G-9023, Saint Louis, Missouri, USA) was applied for 2 hours, at room temperature. Thus, sections of each sample were incubated in a wet chamber for 48 hours, at 4 °C with the primary antibodies (Table 2a) in antibody diluent (1,8% NaCl in a 0.01 M sodium phosphate solution containing 0,1% Na-azide). After primary incubation, the sections were washed with PBS and incubated with the specific secondary antibodies (Table 2b) diluted in PBS in a wet chamber for 2 hours at room temperature. After further three washes in PBS, they were transferred for 30 minutes in an avidin-biotin complex solution (ABC Standard, ABC kit Vectastain, Vector Laboratories, Burlingame, CA, USA, PK 6100) and washed again in PBS. Finally, immunoperoxidase was developed using 3,3'-diaminobenzidine (DAB kit Vector Laboratories, Burlingame, CA, USA, BA-9200). The sections were dehydrated in ethanol, passed in xylene and covered with a coverslip using Entellan.



158 The slides of both Masson's trichrome and IP were observed with an optic microscope (Zeiss  
159 Axioplan, Carl Zeiss, Oberkochen, Germany), captured with the microscope Nikon Coolscope  
160 (Nikon, Japan) and subsequently elaborated with the programs Elipsenet 1.20.0 (Nikon, Japan) and  
161 GIMP 2 (GNU Image Manipulation Program 2.10).

162 For the IF procedure, slides were placed in a wet chamber. A first PBS wash was performed to  
163 rehydrate the sections. A Blocking Serum solution (0,5% Triton X-100, 10% Normal Goat serum,  
164 NGS, Vector, Burlingame, CA, USA, in PBS) or 10% Normal Donkey Serum (NDS, Jackson, Bar  
165 Harbor, Maine, USA) was used at room temperature for 2 hours. Then, the sections of each sample  
166 were incubated in a wet chamber for 48 hours, at 4 °C, with the primary antibodies (Table 2a) in  
167 antibody diluent. After 48 hours, the sections were washed with PBS and either pure NGS or 10%  
168 NDS, (5 x 10 minutes on a stirrer). Next, the sections were incubated for 3 hours, at room temperature,  
169 with specific secondary antibodies (Table 2b), diluted in PBS. After further five 10-minute washes in  
170 PBS, the slides were air dried and prepared with glycerol buffered with 0,5 M sodium carbonate (pH  
171 8,6) to be finally sealed with nail polish.

172 The slides obtained were observed under an epifluorescence optical microscope (Axioplan, Carl  
173 Zeiss, Oberkochen, Germany), equipped with a system of filters that allowed the distinction of the  
174 fluorescence FITC (given by fluorescein) from Alexa 594 fluorescence. The images were acquired  
175 using a digital camera and DMC 2 software (Polaroid Corporation, Cambridge, MA, USA). The  
176 images were processed using Adobe Photoshop (Adobe Systems, San Jose, CA, USA).

177

178 **Table 2a:** List of the primary antibodies used for immunoperoxidase (IP) or immunofluorescence  
179 (IF).

| Primary antibody                              | Used for | Immunogen /host   | Supplier  | Dilution | Antibody RRID  | Validation                     |
|---|----------|-------------------|---|----------|----------------|--------------------------------|
| <b>Protein Gene Product 9.5 (PGP 9.5)</b>     | IP       | Polyclonal rabbit | Millipore, Temecula, CA, USA                              | 1:500    | AB_91019       | PMID:19296476                  |
|   | IF       |                   |   | 1:1000   |                |                                |
| <b>Substance P (SP)</b>                       | IP       | Polyclonal rabbit | Immunostar, Hudson, WI, USA                               | 1:1000   | AB_572266      | PMID:10087030<br>PMID:10196365 |
|   | IF       | Monoclonal rat    | Fitzgerald Industries International, North Acton, MA, USA | 1:200    | AB_2313816     | PMID:22740069<br>PMID:26713509 |
| <b>Calcitonin Gene Related Peptide (CGRP)</b> | IP/IF    | Monoclonal mouse  | Santa Cruz Biotechnology Inc., CA, USA                    | 1:200    | AB_2259462     | PMID:30971286<br>PMID:29943954 |
|   | IF       | Polyclonal rabbit | Peninsula Laboratories Inc., San Carlos, CA, USA          | 1:1000   | AB_2313775     | PMID:18186028<br>PMID:28680400 |
| <b>Human Tyrosine</b>                         | IP/IF    | Monoclonal mouse  | Monosan, Uden, Netherlands                                | 1:50     | ID: MONX10786* | PMID:29615733                  |

|   |       |                   |                                   |        |           |                                |
|---|-------|-------------------|-----------------------------------|--------|-----------|--------------------------------|
| <b>Hydroxylase (TH)</b>                 |       |                   |                                   |        |           |                                |
| <b>Neurofilament 200kDa (NF 200kDa)</b> | IP/IF | Monoclonal rabbit | Sigma, Saint Louis, Missouri, USA | 1:1000 | AB_477272 | PMID:18022951<br>PMID:19937712 |

**Table 2b:** List of the secondary antibodies used for immunoperoxidase (IP) or immunofluorescence (IF).

| Secondary antibody              | Used for | Immunogen /host | Supplier                                   | Dilution | Antibody RRID | Validation                     |
|---------------------------------|----------|-----------------|--|----------|---------------|--------------------------------|
| <b>Biotinylated Anti-Rabbit</b> | IP       | Goat            | Vector Laboratories, Burlingame, CA, USA   | 10 µg/ml | AB_2313606    | PMID:19127523<br>PMID:23766132 |
| <b>Anti-Mouse</b>               | IP       | Goat            | Vector Laboratories, Burlingame, CA, USA   | 10 µg/ml | AB_2336171    | PMID:23766132<br>PMID:25057794 |
| <b>Anti-Mouse Alexa 594</b>     | IF       | Goat            | Thermo Fisher Scientific, Waltham, MA, USA | 1:200    | AB_141372     | PMID:23913443<br>PMID:25057190 |
| <b>Anti-Rat Alexa 594</b>       | IF       | Donkey          | Thermo Fisher Scientific, Waltham, MA, USA | 1:200    | AB_2535795    | PMID:25933105<br>PMID:28089909 |
| <b>Anti-Rabbit-FITC</b>         | IF       | Goat            | Calbiochem, Darmstadt, Germany             | 1:100    | ID: 401314*   | PMID:29615733                  |

\*Antibody RRID are universally identified codes and were taken from the website the antibody registry (<https://antibodyregistry.org/>) which integrated the antibody database of the *Journal of Comparative Neurology*. For each antibody, there is at least one publication correlated to a unique PMID (PubMed Identifier). For the antibodies whose lot number are MONX10786 and 401314, there are still no current RRID available, but the validation appears in one publication (Bombardi et al., 2010).

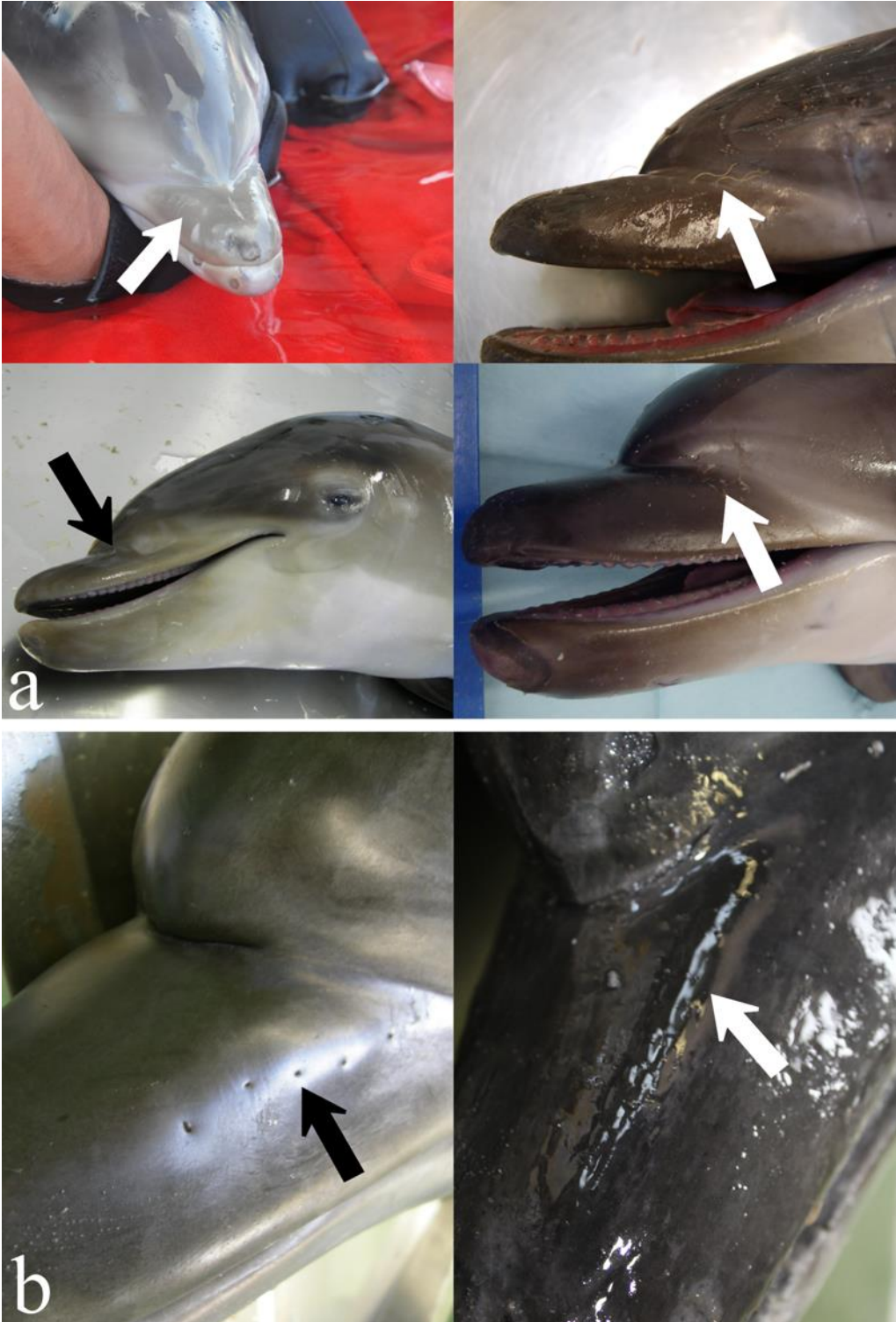


**Figure 1:** Macroscopic images of the rostrum of some specimens of (a, top four) newborn and (b, bottom two) adult bottlenose dolphin. The arrows indicate where the vibrissae emerge from the skin as can be seen in the newborns (a) or the concavity found in the adults (b).

## 195   **Results**

196

### 197   1. Morphology

#### 198   *Newborn dolphins*

199   In the newborns, the external part of the VS was approx. 10 mm long. The FSC of all specimens  
200   consisted of an epidermal and dermal part. The epidermal part comprised the hair with its sheaths,  
201   overlying the dermal venous sinus. The VS originated from the bulb and consisted of three concentric  
202   layers which, from inside to outside, were identified as the medulla, the cortex, both made of  
203   keratinized cells, and the cuticle, which consisted of a simple squamous keratinized epithelium. The  
204   MS and the capsule were fused near the follicle outlet. At the base of the FSC, the bulb resembled a  
205   highly innervated and vascularized dermal papilla (Figure 2a). The VS was wrapped by the inner root  
206   sheath, attached to the cuticle, and the outer root sheath, surrounded by the glassy membrane (Figure  
207   2b). The hair shaft was surrounded by a venous sinus and delimited by a connective tissue capsule.  
208   The sinus comprised internally the MS, in contact with the glassy membrane and externally by a  
209   capsule (Figure 2c).

210   In the slides analyzed, it was never possible to observe either a ringwulst or a ring sinus. Furthermore,  
211   no muscle fiber or gland was present around the follicle.

212

#### 213   *Adult dolphins*

214   In the adults, the VS was present but did not reach the skin surface. Apart from this feature, the FSC  
215   of the adult dolphins showed the same structure of those of the newborns.

216

### 217   2. Innervation

218   Anti-PGP 9.5 immunoreactive (-ir), anti-NF 200-ir, anti-TH-ir and anti-SP-ir nerve fibers were  
219   evident in all the samples. No anti-CGRP-ir fibers were observed.

#### 220   *Newborn dolphins*

221   PGP 9.5-ir fibers penetrated the FSC at the level of the hair bulb, and yielded an intricate arborized  
222   network of ramifications (Figure 3a, b). The nerve fibers protruded at various levels in the  
223   mesenchymal sheath, giving rise to button-like terminations characterizing MNEs (Figure 3c). They  
224   derived from large and medium-sized fibers that ran to form clusters of button-like endings with a  
225   smooth and regular surface, between which fine spiral-like fibers were present (Figure 3d).

226   NF 200-ir fibers were also detected penetrating the bulb (Figure 3e), first running parallel to the VS  
227   and then entering at different levels along the follicle (Figure 3f). Nerve fibers of different calibers

were distributed along the VS, progressing either in a straight line or along a winding path until they reached the top of the FSC (Figure 3f).

Numerous nerve fibers were observed in transversal sections of the FSC, from the hair bulb to the apex (Figure 4). These fibers innervated the hair bulb (Figure 4b, c) and sent small groups of axons to surround the follicle (Figure 4d, e), ending into MNEs (Figure 4f). Some of these axons penetrated the venous sinus, ran along the trabeculae (Figure 4g) and ended at the MS that wrapped the VS with MNEs (Figure 4h). This rich innervation was evident in all transverse sections up to the outlet of the vibrissa (Figure 4i). We did not identify other receptors with certainty and, as mentioned above, most fibers seemed to end as FNEs.

SP-ir fibers ran either grouped in bundles or alone close to blood vessels (Figure 5a, b). Double immunofluorescence for PGP 9.5 and TH showed that PGP 9.5-ir fibers were qualitatively four-fold the TH-ir fibers (Figure 5c, d). TH-ir fibers were mainly located around the blood vessels, and sometimes presented a tortuous pattern. They contained thin-caliber axons that ran first on the surface of the adventitia and then penetrated the wall (Figure 5e). Few TH-ir fibers were found at the base of the bulb and in the MS (Figure 5f).

#### *Adult dolphins*

Immunohistochemical results in adult dolphins showed the same general pattern of that of newborns, with some notable exceptions. PGP 9.5-ir and NF 200-ir nerve fibers were clear (Figure 6a-c) and the MNEs bound to the mesenchymal sheath were smaller in adults (Figure 6d). SP reactivity was found in large caliber fibers near the dermo-epidermal junction (Figure 7a), where they ran parallel to the skin before bending towards the FSC and ending as FNEs (Figure 7b). TH-ir fibers were rarer. Very thin TH-ir fibers were present in the trabeculae of the venous sinus and the mesenchymal sheath ending with isolated oval corpuscles (Figure 7c-e).



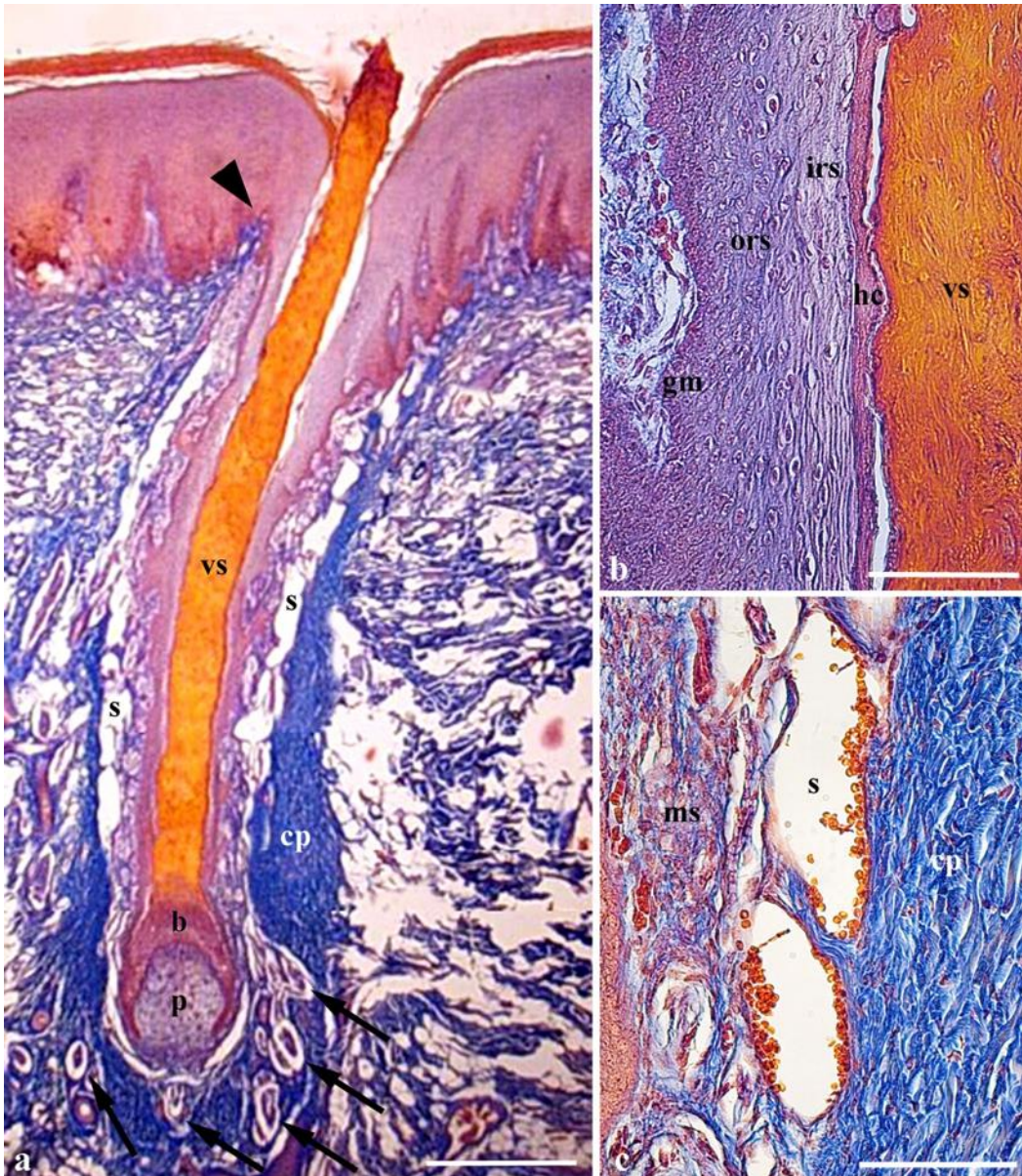


**Figure 2** – Longitudinal section of a typical FSC in newborn bottlenose dolphin. a. The vibrissa is surrounded by a venous sinus (s). A capsule (cp) envelops the complex. Several nerves (arrows) reach the root of the vibrissa. The arrowhead indicates the fusion between the capsule and mesenchymal sheath. b. Detail at higher magnification of the epidermal components. c. Detail at higher magnification of the dermal components. b, bulb; cp, capsule; gm, glassy membrane; irs, inner root sheath; ms, mesenchymal sheath; ors, outer root sheath; p, papilla; s, venous sinus; vs, vibrissal shaft. Masson's Trichrome stain. Scale bars: a = 1 mm; b, c = 100  $\mu$ m.



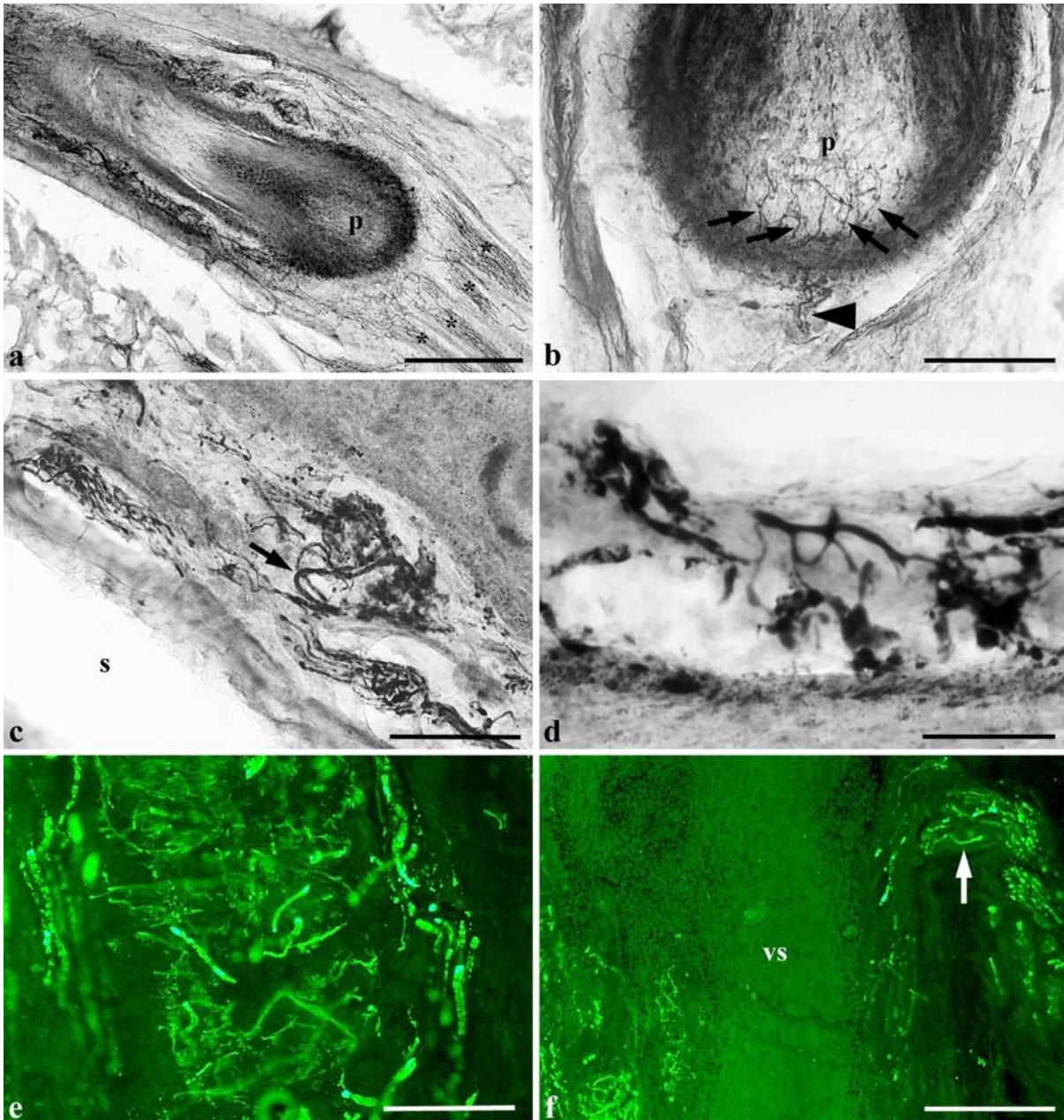


**Figure 3** – Innervation of the FSC in a newborn bottlenose dolphin. The nerve fibers were immunolabelled for PGP 9.5 (a-d) and NF200kD (e, f). a. Several PGP 9.5-ir nerve bundles (asterisks) reach the root of the vibrissa. p, papilla. b. Few thin-caliber fibers (arrowhead) enter the papilla (p) and terminate as free nerve endings (arrows). c. In the mesenchymal sheath, some nerve fibers (arrow) give rise to MNEs (asterisks). d. High magnification showing MNEs. Note the characteristic button-like endings. e. The dense network of nerve fibers around the bulb. f. A nerve bundle penetrate the FSC laterally. vs, vibrissal shaft. Scale bars: a, e =100  $\mu$ m; b, c, f = 200  $\mu$ m; d = 50  $\mu$ m.

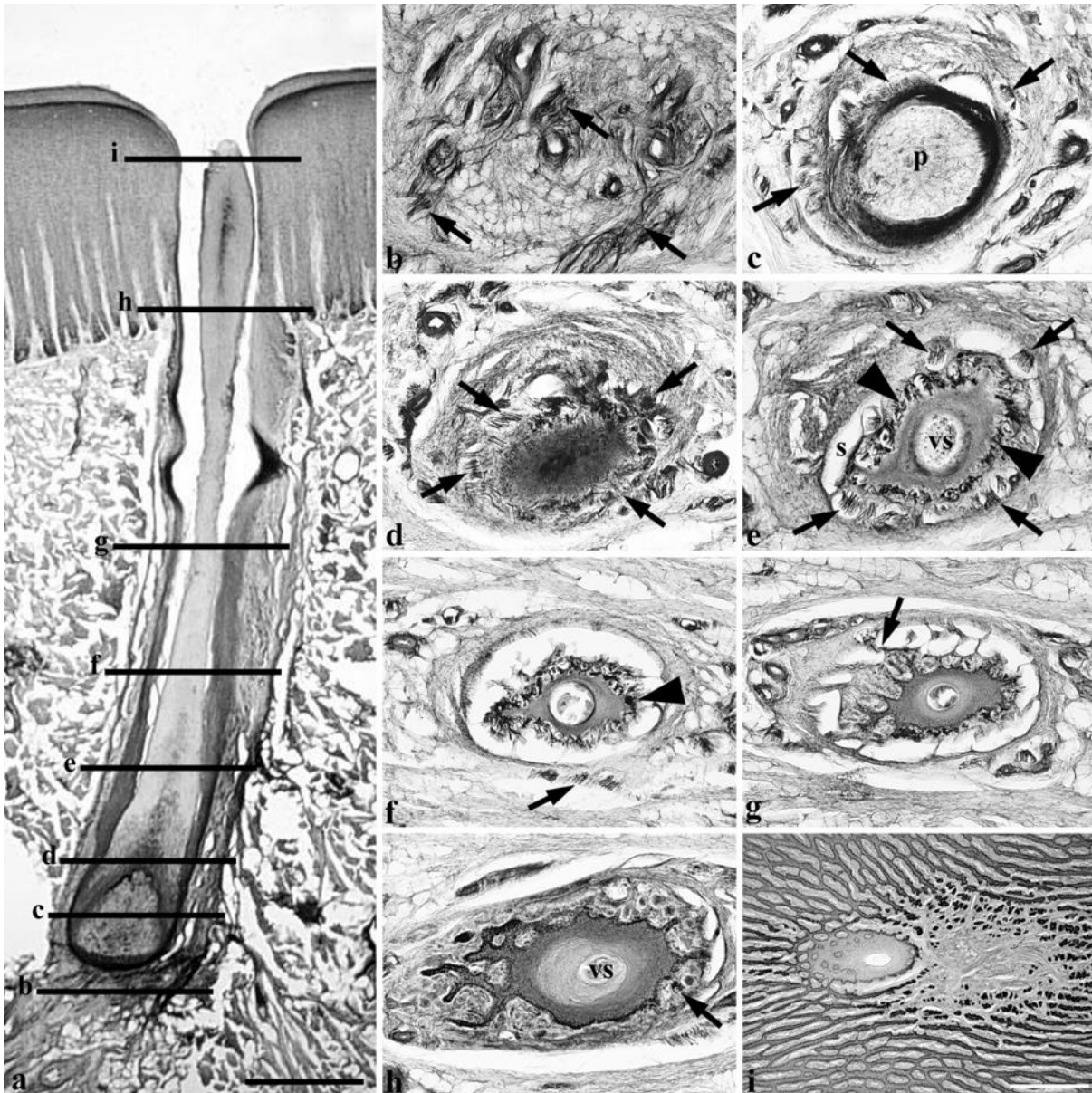


**Figure 4** – Longitudinal (a) and transverse (b-i) sections (b) of FSC in newborn bottlenose dolphin showing the innervation at different levels from the basal (b) to the apical (i). The nerve fibers were immunolabelled with antibodies to PGP 9.5. b. Some nerves (arrows) reach the root of the vibrissa. c. The nerves break into several fascicles (arrows) that ascend close to the papilla (p). d. The nerve fibers (arrows) surround the follicle. e. Some nerve fibers (arrows) penetrate the venous sinus (s) and branch in the mesenchymal sheath (arrowhead). vs, vibrissal shaft. f. Some fibers terminate on MNEs (arrowhead), while others continue along the FSC (arrow). g. A nerve fiber (arrow) passes through one of numerous trabeculae of the venous sinus. h. At the level of dermo-epidermal border, the nerve fibers disappear but the MNEs are still present (arrow). i. Section through the skin and the dermal papilla. Scale bars: a = 1 mm; b-h = same magnification of i; i = 350  $\mu$ m.



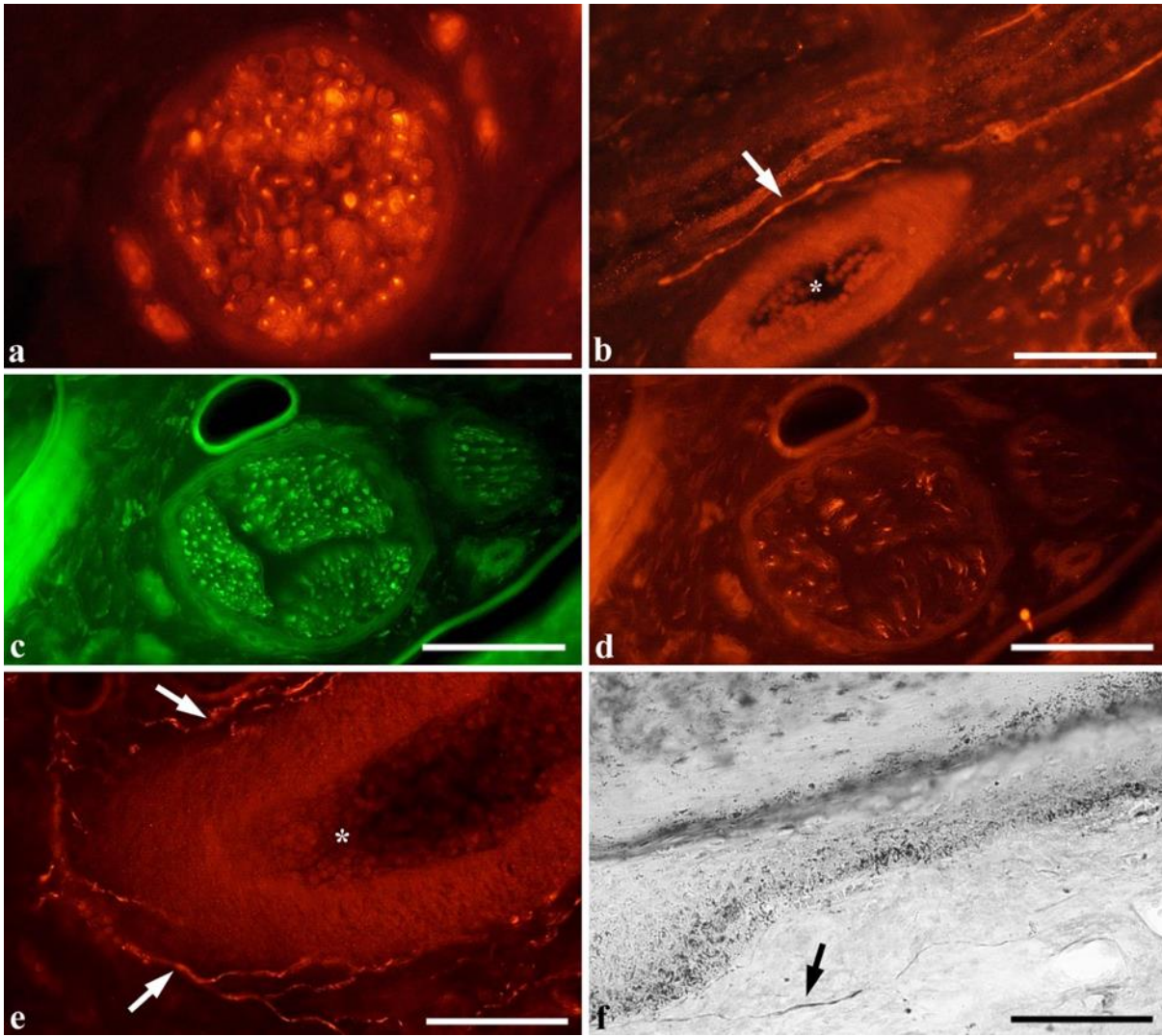


**Figure 5** - SP- (a, b) and TH-(c-f) immunoreactive fibers in newborn bottlenose dolphin. a. Transverse section of a nerve bundle showing many immunoreactive fibers. b. A nerve fiber (arrow) runs parallel to a blood vessel (asterisk). c, d. Double immunofluorescence PGP 9.5-FITC (c) / TH-Alexa 594 (d) of a nerve bundle in transverse section. Note the TH immunoreactivity of some fibers. e. Several nerve fibers (arrows) reach the tunica adventitia of a vessel (asterisk). f. A thin fiber run within the ms. Scale bars = 100  $\mu$ m.

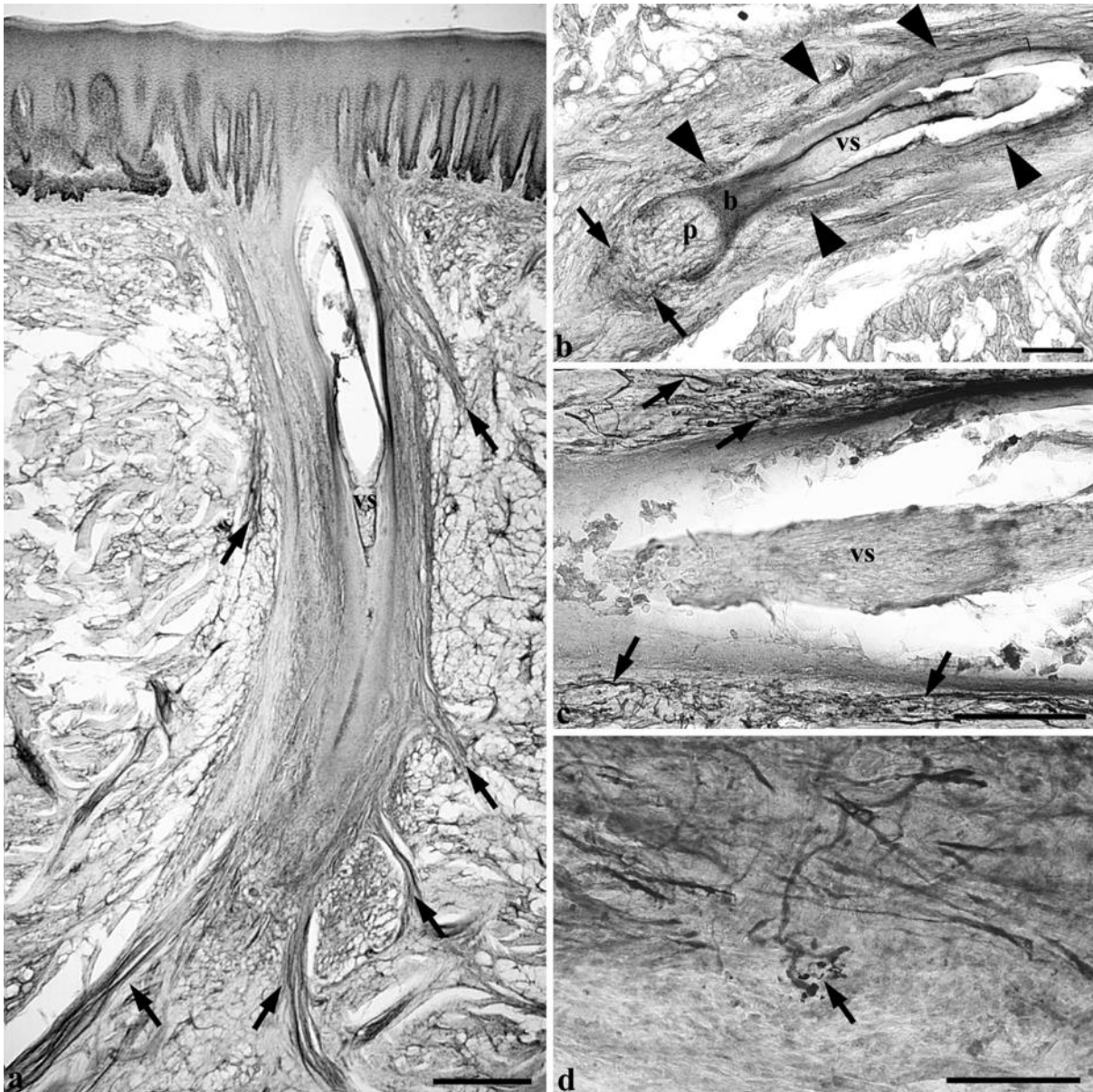


**Figure 6** – Longitudinal sections of FSC in adult bottlenose dolphin. The nerve fibers were immunolabelled for PGP 9.5 (a, b) and NF200kD (c, d). a. Note the six nerve bundles (arrows) reaching the FSC. b. A vibrissa is clearly visible inside the follicle. Some nerve fibers (arrows) reach the bulb, others (arrowheads) run within the ms. b, bulb; p, papilla; vs, vibrissal shaft. c. High magnification showing the rich innervation (arrows) of the ms. d. Detail of a MNE (arrow). Scale bars: a, b = 1 mm; c = 200 μm; d = 100 μm.

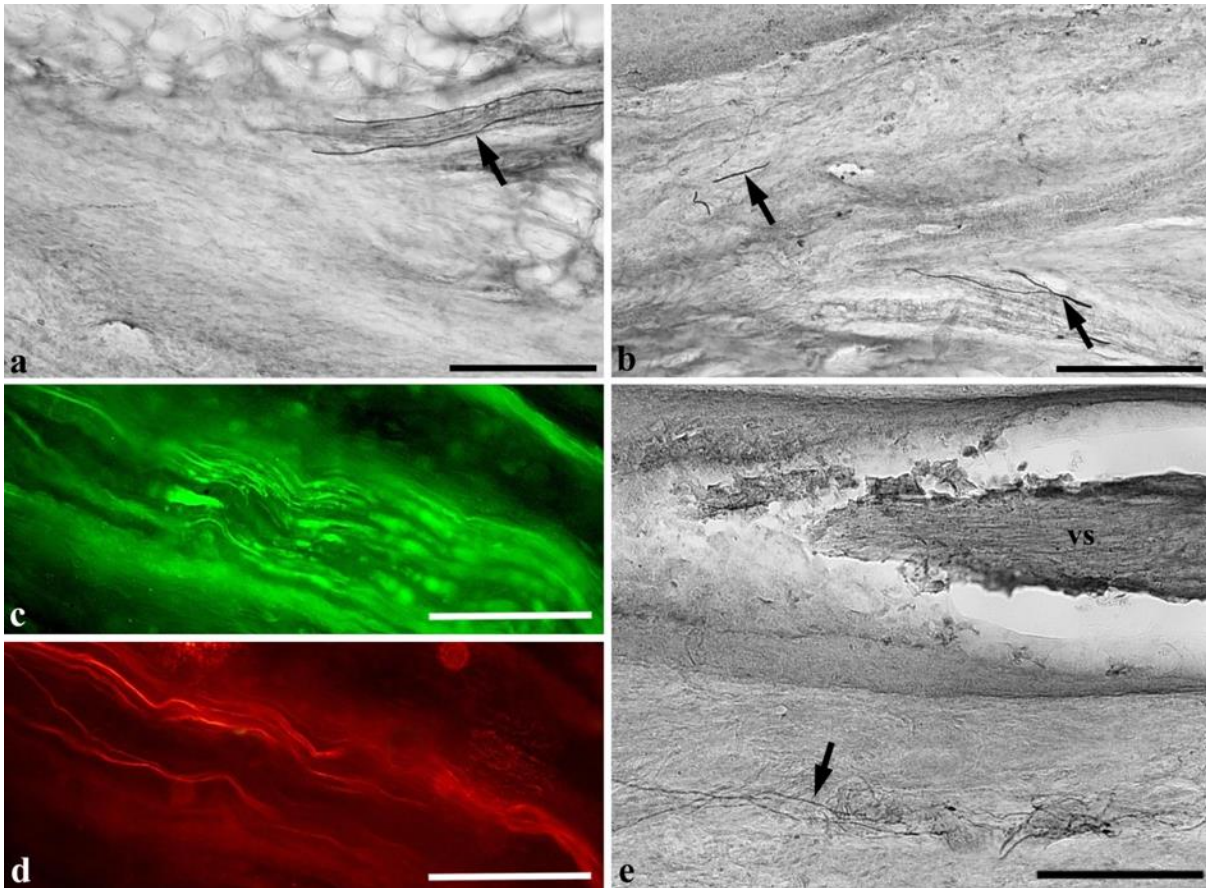


**Figure 7** – SP- (a, b) and TH- (c-e) immunoreactive fibers in an adult bottlenose dolphin. a. Two positive fibers reach the FSC laterally. b. Few nerve fibers in the ms. c, d. Double immunofluorescence PGP 9.5-FITC (c) / TH-Alexa 594 (d) of a large nerve bundle in longitudinal section. Note the few TH-ir fibers. e. Few fibers (arrow) in the ms. Scale bars: a, b, e = 200 μm; c, d = 100 μm.

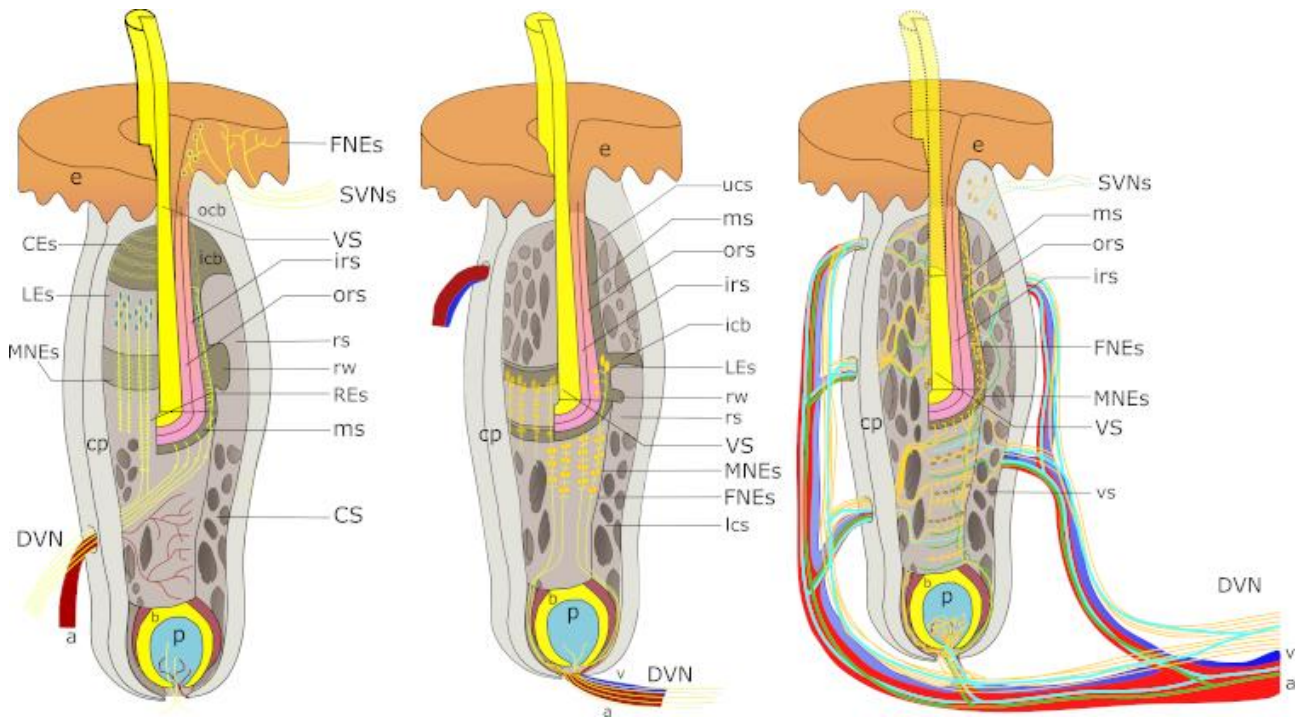
## 306 Discussion

307 In the present work, we describe the morphology and the innervation of FSC of newborn and adult  
308 bottlenose dolphins. Our findings reveal that newborn specimens possess a complete structure divided  
309 in an epidermal and a dermal part, hence the term “follicle-sinus complex” whereas, in adults, the VS  
310 lies within the follicle (Figs. 2, 6). The absence of a ring sinus (ringwulst) of the *erector pili* muscle  
311 and of any kind of associated gland constitutes differences with the vibrissae in terrestrial mammals.  
312 The blood sinus of the bottlenose dolphin consists of just one cavity forming a trabecular net just like  
313 the tammar wallaby (*Macropus eugenii*) (Marotte *et al.*, 1992) and is not divided into two parts as in  
314 terrestrial mammals (Rice *et al.*, 1986, Ebara *et al.*, 2002) or three parts as in pinnipeds (Marshall *et*  
315 *al.*, 2006) (Figure 8).

316 Anti-neuronal antibodies (anti-PGP 9.5, -NF 200, -TH, and -SP) helped to characterize the  
317 innervation of the FSC. Antibodies directed against proteins of the neurofilaments (anti-PGP 9.5, -  
318 NF 200, Figs. 3, 4, 6) identified several fiber bundles which bifurcated from the deep vibrissal nerve  
319 at the bottom of the FSC to reach various heights of the follicle, similarly to what was previously  
320 described in manatees (Sarko *et al.*, 2007). Few fibers were also found at the dermo-epidermal  
321 junction (Figure 4i). Merkel receptors were evenly distributed along the MS of the FSC, although, in  
322 the newborn they were also found at the dermo-epidermal junction (Figs. 3, 4). Since no striated  
323 muscle fibers and no glands were present in the FSC, the nature of the present innervation is likely  
324 somatosensory and derived from the maxillary nerve (V2) of the trigeminal nerve. The V2 runs –  
325 from its exit of the skull base – rostrally to enter the dolphin equivalent of the maxillary foramen and  
326 subsequent canal. The rostralmost fibers of the V2 run as the infraorbital nerve in maxillary canals.  
327 Some fibers of the latter penetrate the maxilla in dorsal direction to provide sensorial innervation to  
328 the skin of the rostrum (Rauschmann 1992). Dolphins possess no movable lips and have virtually no  
329 snout fascia or mimic muscles beyond those, more caudal, that act on the melon, thus implying a  
330 virtual absence of a somato-motor component in the facial nerve this far forward on the face.  
331 Comparisons with other mammals are difficult. Whisking rodents possess the mystacial pad, a  
332 thickening of the snout fascia where mimic muscles, sensory receptors and collagen structures form  
333 a highly developed motor-sensory organ (Haidarliu *et al.*, 2020). In the rat and mouse, a column of  
334 neocortical neurons in the whisker somatosensory cortex (wS1, or barrel cortex) corresponds to each  
335 FSC, with a highly developed layer IV receiving the thalamic afferent (Woolsey and Van der Loos,  
336 1970; Van der Loos and Woolsey, 1973; Van der Loos, 1976; Rice and Van Der Loos, 1977;  
337 Jeanmonod *et al.*, 1981; Pearson *et al.*, 2006; Bosman *et al.*, 2011; Schröder *et al.*, 2020). However,  
338 the barrel cortex is typical of rodents, and is not present in any other species (i.e. mammals of the  
339 genus *Felis* or *Panthera*), even ones which present whisking behavior such as the short-tailed



340 opossum (Waite *et al.*, 1991; Ramamurthy and Krubitzer, 2016). Furthermore, the neocortex of  
 341 dolphins and whales lacks a layer IV and it is currently hypothesized that thalamic projections reach  
 342 layer II instead of IV (for general description see Cozzi *et al.*, 2017), thus making any comparison  
 343 with the highly specialized barrel cortex of rodents difficult. In particular the study by van Kann and  
 344 colleagues (2017) pointed out the main differences in the primary neocortical areas layering between  
 345 the common dolphin, the wild boar and humans.  
 346 The use of antibodies against peptides (SP, CGRP) and against a key enzyme in catecholamine  
 347 synthesis (TH), allowed further characterization of the innervation. SP is involved in nociception, and  
 348 a subpopulation of sensory neurons in the mammalian trigeminal ganglion contains SP, colocalized  
 349 with CGRP (Alvarez *et al.*, 1988, Fundin *et al.*, 1997b; Waite and and Ashwell, 2012). SP-ir neurons  
 350 have also been described in the dorsal root ganglia of bottlenose dolphins (Bombardi *et al.*, 2010).  
 351



352  
 353 **Figure 8** – Schematic drawn representing the main differences between the FSCs of a terrestrial  
 354 mammal (left), pinniped (center) and dolphin (right). On the right, the follicle represented is that of  
 355 the adult as the dotted lines and transparent areas (SVNs and MNEs in the dermo-epidermal junction)  
 356 are of the newborn. In terrestrial mammals the FSC is divided into two halves, the inferior cavernous  
 357 sinus, and the superior ring sinus. Receptors, coming mainly from the deep vibrissal nerve are  
 358 positioned at different heights depending on their sensory nature. In pinnipeds it is instead divided  
 359 into three portions, including an upper cavernous sinus. The fibers, which derive only from the deep  
 360 vibrissal nerve, innervate up to the inner conical body, without reaching the epidermis. Finally, in the  
 361 dolphin, a trabecular component forms a single venous sinus in which the receptors, also deriving  
 362 mainly from the deep vibrissal nerve, are distributed along the follicle until they reach the epidermis  
 363 in the newborn. Also note the TH-ir (green) and SP-ir (light blue) fibers which accompany the blood  
 364 vessels. Abbreviations: VS, vibrissal shaft; e, epidermis; irs, inner root sheath; ors, outer root sheath;  
 365 ms, mesenchymal sheath; ocb, outer conical body; icb, inner conical body; rw, ringwulst; rs, ring  
 366 sinus; cs, cavernous sinus; lcs, lower cavernous sinus; ucs, upper cavernous sinus; c, capsule; p,

367 papilla; b, bulb; DVN, deep vibrissal nerve; SVNs, superficial vibrissal nerves; MNEs, merkel nerve  
368 endings; FNEs, free nerve endings; CEs, circular endings; LEs, lanceolate endings; REs, reticular  
369 endings; a, artery; v, vein; vs, venous sinus.

371 Several SP-ir were located in the dermo-epidermal junction and, deeper lateral to the follicle. Other  
372 SP-ir nerves were also found around the sinus' blood vessels. Both SP and CGRP are vasodilators.  
373 However, the presence of SP-ir fibers within big nerve bundles suggests a nociceptive function while  
374 the presence of SP in thin fibers around blood vessels might indicate a parasympathetic activity on  
375 the vessels of the FSC (Fundin *et al.*, 1997b). No CGRP-ir fiber was detected in the vibrissae of the  
376 dolphins in this study. This absence is difficult to explain from a functional point of view. Indeed,  
377 CGRP has been found in the gastrointestinal tract of the striped dolphin (*Stenella coeruleoalba*)  
378 (Domenighini *et al.*, 1997), and has been proposed to be present in CNS of the bottlenose dolphin  
379 (Rambaldi *et al.*, 2016). Additionally, the presence of this molecule was demonstrated in the FSC of  
380 manatees (Sarko *et al.*, 2007). Therefore, the apparent absence of CGRP in the FSC of the bottlenose  
381 dolphin could be due to a loss of nociceptive function or different trigeminal organization.

382 TH-ir fibers consisted of thin branches located around the surface of the blood vessels connecting to  
383 the sinus, even though some elements were found also in the MS and trabeculae. Considering their  
384 peripheral location, TH-ir fibers are indicative of a noradrenergic sympathetic innervation derived  
385 from the cranial [superior] cervical ganglion. In mammals, sympathetic fibers follow both the external  
386 and internal carotid arteries. From the former, fibers then run along the infraorbital artery. However,  
387 the internal carotid artery obliterates early in postnatal life in dolphins (Boenninghaus, 1903; Cozzi  
388 *et al.*, 2017), as in many Cetartiodactyls. Therefore, the precise route of the TH-ir that was observed  
389 in the FCS of dolphins remains to be ascertained. It may be possible that the internal carotid artery  
390 develops in the odontocete embryo to guide the growing sympathetic fibers from the cervical ganglion  
391 since it is known that the axonal outgrowth of mammalian sympathetic precursors proceeds in  
392 dependence and thus in parallel to the development of the internal carotid artery (reviewed in Kameda  
393 2020). Thus, possibly only after the sympathetic fibers have found their route, the internal carotid  
394 artery obliterates in odontocetes. Alternatively, these fibers in cetaceans may rely exclusively on the  
395 external carotid path.

396 Contrarily to what was reported by Yablokov *et al.* (1972), we were able to confirm the presence of  
397 the VS in adult specimens, as was previously described by Palmer and Weddell (1964). In all the  
398 adult animals analyzed in the present study, the FSC was complete, i.e. the epidermal and dermal  
399 components were discernable, and the VS was still present, albeit only in the follicle. In fact, the hair  
400 papillae maintained the same morphology found in the newborns. Moreover, the VS did not have the  
401 aspect of a formless cluster due to the epithelial regeneration. Since the papilla is responsible for the

production of the VS's components, a lack of this structure can justify the absence of the VS in the adult Guiana dolphin, in which it had transformed into an agglomeration of fat cells (Czech-Damal *et al.*, 2012). Interestingly, we found MNEs and FNEs but no other receptor, which is coherent with what was described in the Guiana dolphin (Czech-Damal *et al.*, 2012). In the absence of other markers (e.g. anti-S100 protein), it however remains impossible to rule out the existence of other nerve endings such as Pacini corpuscles.

The Guiana dolphin is in fact very similar to the ubiquitous bottlenose dolphin in general body morphology and proportions, although somewhat smaller. Yet, the preferred habitat of the Guiana dolphin is estuarine and coastal, while bottlenose dolphins are distributed worldwide and live both along coastlines and in the high seas. The FSC complex in Guiana dolphins has been linked to the sensitivity to electric fields generated by prey burrowed in sand or hidden by murky waters (Czech-Damal *et al.*, 2012, 2013). A progressive morphological adaptation to different specific environments over time may be the explanation to the differences in the structure of the FSC in those two similarly sized species. Whether the evolution was towards a loss or a gain of function remains unclear.

Based on the absence in dolphins of morphological features typical of terrestrial mammals with vibrissae, i.e. the absence of a wide range of receptors, the mystacial pad or the barrel cortex, we can infer that the FSC of dolphins are relatively rigid structures, with a sensitivity potentially reduced which does not allow perception of dynamic changes the way fully formed whiskers do. Yet, since the vibrissae persist in newborn dolphins, contrarily to other structures lost during fetal growth (pelvic limbs, to name the most striking difference with land mammals) it is possible that the vibrissae play a role in the early postnatal life, in the days immediately following parturition.

Pinniped mothers recognize their newborn mostly through olfaction while the newborn, from the first minutes of life, vocalizes for most of the first day, a behaviour that diminishes gradually afterwards (Trillmich, 1981). Underwater, this kind of recognition is almost impossible to dolphins since they cannot smell (Cozzi *et al.*, 2017). As proposed by Cozzi *et al.* (2012, 2015), an evolutionary adaptation in cetaceans to an immediate recognition is the early ossification of the tympanic bulla which would allow the newborn to locate the mother's vocalizations and help it in postpartum period. However, full echolocation capacities are likely not to fully develop until month 1-3 after birth (Harder *et al.*, 2016); and while it is difficult to think that vibrissae may act for this recognition, it is more plausible that it could allow the newborn to find the opening of the nipples immediately after birth, thanks to the rich SP innervation and vasomodulation regulated by the TH-ir plexus (Fundin *et al.*, 1997b; Maklad, 2004).

A VS is still present within the FSC in the adult dolphin and the innervation remains relatively developed. The original tactile function of the FSC may lose value in the growing dolphins that, later

436 in life, may rely on different sensory modalities to interact with their mother and the rest of the pod.  
437 This organ could act as a proprioceptor as suggested by Yablokov *et al.* (1972). The VS could be  
438 sensitive to low frequency oscillations and water movements caused by head rotation and would  
439 consequently activate the receptors that provide this information to the central nervous system. This  
440 would allow the dolphin to always have a perception of the angular position of the head. Nervous  
441 fibers could modify the pressure inside the venous system and help maintain thermoregulation and  
442 modify the threshold of the receptors (Fundin *et al.*, 1997b). This idea does not preclude that the  
443 structure found by Czech-Damal and colleagues (2012) in the Guiana dolphin could function as an  
444 electroreceptor. However, to confirm or reject this hypothesis, further psychophysical experiments  
445 should be conducted in the bottlenose dolphin.



446 **Authors contributions :**

447 TG, AG, JMG and BC designed the study, TG, AG, CT and MDS acquired and analyzed the data.  
448 TG, AG, JMG and BC wrote the draft. AG, SdV and SH critically revised the manuscript. All  
449 authors approved the article.

450 **Bibliography:**

- 451 Alvarez, F. J., Cervantes, C., Blanco, I. et al. (1988) ‘Presence of calcitonin gene-related peptide  
452 (CGRP) and substance P (SP) immunoreactivity in intraepidermal free nerve endings of cat  
453 skin’, *Brain research*, 442(2), pp. 391-395. doi: 10.1016/0006-8993(88)91532-6.
- 454 Bombardi, C., Grandis, A., Nenzi, A., Giurisato, M. and Cozzi, B. (2010) ‘Immunohistochemical  
455 localization of substance P and cholecystokinin in the dorsal root ganglia and spinal cord of the  
456 bottlenose dolphin (*Tursiops truncatus*)’ *The Anatomical Record: Advances in Integrative Anatomy  
457 and Evolutionary Biology*, 293(3), pp. 477-484. doi: 10.1002/ar.20975.
- 458 Boenninghaus, G. (1903). *Das Ohr des Zahnwales, zugleich ein Beitrag zur Theorie der Schalleitung:  
459 eine biologische Studie*. Fischer.
- 460 Bosman, L. W. J., Houweling A. R., Owens, C. B. et al. (2011) ‘Anatomical pathways involved in  
461 generating and sensing rhythmic whisker movements’, *Frontiers in Integrative Neuroscience*, 5, pp.  
462 1–28. doi: 10.3389/fnint.2011.00053
- 463 Cave, A. J. E. (1969) ‘Hairs and vibrissae in the Rhinocerotidae’ *Journal of Zoology*, 157(2), pp.  
464 247–257. doi:10.1111/j.1469-7998.1969.tb01700.x
- 465 Chernova, O. F. (2006) ‘Evolutionary aspects of hair polymorphism’, *Biology Bulletin*, 33(1), pp. 43-  
466 52. doi: 10.1134/S1062359006010067
- 467 Cozzi, B., Podesta, M., Mazzariol, S. and Zotti, A. (2012) ‘Fetal and early post-natal mineralization  
468 of the tympanic bulla in fin whales may reveal a hitherto undiscovered evolutionary trait’, *PloS  
469 One*, 7(5), e37110. doi: 10.1371/journal.pone.0037110.
- 470 Cozzi, B., Podestà, M., Vaccaro, C. et al. (2015) ‘Precocious ossification of the tympanoperiotic bone  
471 in fetal and newborn dolphins: an evolutionary adaptation to the aquatic environment?’, *The  
472 Anatomical Record*, 298(7), pp. 1294-1300. doi: 10.1002/ar.23120
- 473 Cozzi, B., Huggenberger, S. and Oelschläger, H.A. (2017) *Anatomy of dolphins: insights into body  
474 structure and function*. 1<sup>st</sup> ed. London: Academic Press.
- 475 Czech-Damal, N. U., Liebschner, A., Miersch, L. et al. (2012) ‘Electroreception in the Guiana dolphin  
476 (*Sotalia guianensis*)’, *Proceedings of the Royal Society B: Biological Sciences*, 279(1729), pp. 663–  
477 668. doi: 10.1098/rspb.2011.1127.
- 478 Czech-Damal, N. U., Dehnhardt, G., Manger, P. and Hanke, W. (2013) ‘Passive electroreception in  
479 aquatic mammals’, *Journal of Comparative Physiology A: Neuroethology, Sensory, Neural, and  
480 Behavioral Physiology*, 199(6), pp. 555–563. doi: 10.1007/s00359-012-0780-8.
- 481 Dehnhardt G. and Hanke, F. D. (2017). ‘Whiskers’ in Würsig, B., Thewissen, J. G. M. and Kovacs,  
482 K. M. (Eds) *Encyclopedia of marine mammals*. 3<sup>rd</sup> ed. London: Academic Press. pp. 1074-1076.

483 Domeneghini, C., Massoletti, P., and Arrighi, S. (1997) 'Localization of regulatory peptides in the  
 484 gastrointestinal tract of the striped dolphin, *Stenella coeruleoalba* (Mammalia: Cetacea). An  
 485 immunohistochemical study' *European Journal of Histochemistry*, 41(4), pp. 285-300. PMID:  
 486 9491315.

487 Dougill, G., Starosin, E.L., Milne, A.O., van der Heijden, G.H.M., Goss, V.G.A., and Grant, R.A.  
 488 (2020) Ecomorphology reveals Euler spiral of mammalian whiskers. *Journal of Morphology*, DOI:  
 489 10.1002/jmor.21246.

490 Ebara, S., Kumamoto, K., Matsuura, T., Mazurkiewicz, J.E. and Rice, F.L. (2002) 'Similarities and  
 491 differences in the innervation of mystacial vibrissal follicle-sinus complexes in the rat and cat: A  
 492 confocal microscopic study', *Journal of Comparative Neurology*, 449(2), pp. 103–119. doi:  
 493 10.1002/cne.10277.

494 Fundin, B. T., Arvidsson, J. and Rice, F. L. (1995) 'Innervation of nonmystacial vibrissae in the adult  
 495 rat', *Journal of Comparative Neurology*, 357(4), pp. 501-512. doi: 10.1002/cne.903570402.

496 Fundin, B. T., Bergman, E. and Ulfhake, B. (1997a) 'Alterations in mystacial pad innervation in the  
 497 aged rat', *Experimental brain research*, 117(2), pp. 324-340. doi: 10.1007/s002210050226.

498 Fundin, B. T., Pfaller, K. and Rice, F. L. (1997b) 'Different distributions of the sensory and autonomic  
 499 innervation among the microvasculature of the rat mystacial pad', *Journal of Comparative*  
 500 *Neurology*, 389(4), pp. 545–568. doi: 10.1002/(SICI)1096-9861(19971229)389:4<545::AID-  
 501 CNE1>3.0.CO;2-0.

502 Haidarliu, S., Simony, E., Golomb, D. and Ahissar, E. (2010) 'Muscle architecture in the mystacial  
 503 pad of the rat', *Anatomical Record*, 293(7), pp. 1192–1206. doi: 10.1002/ar.21156.

504 Haidarliu, S., Bagdasaria, K., Sardonicus, S. and Ahissar, E. (2020) 'Interaction between muscles and  
 505 fascia in the mystacial pad of whisking rodents', *Anatomical Record* Accepted Author Manuscript.  
 506 doi: [10.1002/ar.24409](https://doi.org/10.1002/ar.24409).

507 Harder, J.H., Hill, H.M., Dudzinski, K.M. et al. (2016) 'The development of echolocation in  
 508 bottlenose dolphins', *International Journal of Comparative Psychology*, 29(1). Retrieved from  
 509 <https://escholarship.org/uc/item/0q22949q>

510 Herfst, L. J. and Brecht, M. (2008) 'Whisker movements evoked by stimulation of single motor  
 511 neurons in the facial nucleus of the rat', *Journal of Neurophysiology*, 99(6), pp. 2821–2832. doi:  
 512 10.1152/jn.01014.2007.

513 Hyvärinen, H. (1989) 'Diving in darkness: whiskers as sense organs of the ringed seal (*Phoca hispida*  
 514 *saimensis*)', *Journal of Zoology*, 218(4), pp. 663-678. doi: 10.1111/j.1469-7998.1989.tb05008.x.

515 Hyvärinen, H. (1995). 'Structure and function of the vibrissae of the ringed seal (*Phoca hispida* L.)'  
516 in R. A. Kastelein, J.A. Thomas, and P. E. Nachtigall (Eds.) *Sensory systems of aquatic mammals*.  
517 Woerden, The Netherlands: De Spil Publishers, pp. 429–445.

518 Hyvärinen, H., Palviainen, A., Strandberg, U. and Holopainen, I.J. (2010) 'Aquatic environment and  
519 differentiation of vibrissae: Comparison of sinus hair systems of ringed seal, otter and pole cat',  
520 *Brain, Behavior and Evolution*, 74(4), pp. 268–279. doi: 10.1159/000264662.

521 Hollis, D.E., and Lyne, A.G. (1974) 'Innervation of vibrissa follicles in the marsupial *Trichosurus*  
522 *vulpecula*' *Australian Journal of Zoology*, 22(3), pp. 263. doi:10.1071/zo9740263

523 Kameda, Y. (2020) 'Molecular and cellular mechanisms of the organogenesis and development of  
524 the mammalian carotid body', *Developmental Dynamics*, 249(5), pp. 592–609. doi:  
525 10.1002/dvdy.144.

526 Ling, J.K. (1966) 'The skin and hair of the southern elephant seal, *Mirounga leonina* (Linn.) I. The  
527 facial vibrissae', *Australian Journal of Zoology*, pp. 855–866. doi: 10.1071/ZO9660855.

528 Ling, J.K. (1977). 'Vibrissae of marine mammals' in Harrison, R. J. (Ed.) *Functional Anatomy of*  
529 *Marine Mammals. Vol. 3*. London: Academic Press. pp. 387–415.

530 Lyne, A. G. (1958) 'The systematic and adaptive significance of the vibrissae in the marsupialia'  
531 *Proceedings of the Zoological Society of London*, 133(1), pp. 79–133. doi:10.1111/j.1469-  
532 7998.1959.tb05555.x

533 Maklad, A., Fritsch, B. and Hansen, L. A. (2004) 'Innervation of the maxillary vibrissae in mice as  
534 revealed by anterograde and retrograde tract tracing', *Cell and Tissue Research*, 315(2), pp. 167–  
535 180. doi: 10.1007/s00441-003-0816-z.

536 Marotte, L. R., Rice, F. L., and Waite, P. M. (1992) 'The morphology and innervation of facial  
537 vibrissae in the tammar wallaby, *Macropus eugenii*' *Journal of anatomy*, 180(Pt 3), pp. 401-417.  
538 PMID: 1487434

539 Marshall, C.D., Amin, H., Kovacs, K.M. and Lydersen, C. (2006) 'Microstructure and innervation of  
540 the mystacial vibrissal follicle-sinus complex in bearded seals, *Erignathus barbatus* (Pinnipedia:  
541 Phocidae)', *The Anatomical Record Part A: Discoveries in Molecular, Cellular, and Evolutionary*  
542 *Biology: An Official Publication of the American Association of Anatomists*, 288(1), pp. 13-25. doi:  
543 10.1002/ar.a.20273

544 Muchlinski, M. N. (2010) 'A comparative analysis of vibrissa count and infraorbital foramen area in  
545 primates and other mammals', *Journal of human evolution*, 58(6), pp. 447-473. doi:  
546 10.1016/j.jhevol.2010.01.012.

547 Palmer, E. and Weddell, G. (1964) 'The relationship between structure innervation and function of  
548 the skin of the Bottlenose dolphin (*Tursiops truncatus*)', *Proceedings of the Zoological Society of*  
549 *London*, 143(4), pp: 553-568. doi: 10.1111/j.1469-7998.1964.tb03881.x.

550 Park, T. J., Comer, C., Carol, A., Lu, Y., Hong, H. S. and Rice, F. L. (2003) 'Somatosensory  
551 organization and behavior in naked mole-rats: II. Peripheral structures, innervation, and selective  
552 lack of neuropeptides associated with thermoregulation and pain', *Journal of comparative*  
553 *neurology*, 465(1), pp: 104-120. doi: 10.1002/cne.10824.

554 Pearson, M., Nibouche, M., Pipe, A.G. et al. (2006) A biologically inspired FPGA based  
555 implementation of a tactile sensory system for object recognition and texture discrimination. In 2006  
556 International Conference on Field Programmable Logic and Applications (pp. 1-4). IEEE.

557 Van der Loos, H., and Woolsey, T. A. (1973) 'Somatosensory cortex: structural alterations following  
558 early injury to sense organs.' *Science*, 179(4071), pp. 395-398. doi: 10.1126/science.179.4071.395.

559 Van Der Loos, H. (1976) 'Barreloids in mouse somatosensory thalamus' *Neuroscience letters*, 2(1),  
560 pp. 1-6. doi: 10.1016/0304-3940(76)90036-7.

561 Rice, F. L., and Van Der Loos, H. (1977) 'Development of the barrels and barrel field in the  
562 somatosensory cortex of the mouse' *Journal of Comparative Neurology*, 171(4), pp. 545-560. doi:  
563 10.1002/cne.901710408.

564 Jeanmonod, D., Rice, F. L., and Van der Loos, H. (1981) 'Mouse somatosensory cortex: alterations  
565 in the barrelfield following receptor injury at different early postnatal ages' *Neuroscience*, 6(8), pp.  
566 1503-1535. doi: 10.1016/0306-4522(81)90222-0.

567 Ramamurthy, D. L., and Krubitzer, L. A. (2016) 'The evolution of whisker-mediated somatosensation  
568 in mammals: Sensory processing in barrelless S1 cortex of a marsupial, *Monodelphis domestica*'  
569 *Journal of Comparative Neurology*, 524(17), pp. 3587-3613. doi: 10.1002/cne.24018.

570 Rambaldi, A., Grandis, A., Mazzoni, M., Tagliavia, C., Clavenzani, P., Cozzi, B., and Bombardi, C.  
571 (2016) 'Calcitonin Gene-Related Peptide (CGRP) expression in the spinal cord and spinal ganglia  
572 of the Bottlenose Dolphin (*Tursiops truncatus*)' *Annals of Anatomy-Anatomischer Anzeiger*,  
573 100(207), pp. 124. doi: 10.1016/j.aanat.2016.04.023.

574 Rauschmann, M.A. (1992). 'Morphologie des Kopfes beim Schlanken Delphin *Stenella attenuata* mit  
575 besonderer Berücksichtigung der Hirnnerven' (Inaugural-Dissertation, Fachbereich Medizin).  
576 Johann Wolfgang Goethe-Universität, Frankfurt am Main.

577 Reep, R. L., Marshall, C. D., Stoll, M. L. and Whitaker, D. M. (1998) 'Distribution and innervation  
578 of facial bristles and hairs in the Florida manatee (*Trichechus manatus latirostris*)', *Marine Mammal*  
579 *Science*, 14(2), pp. 257-273. doi: 10.1111/j.1748-7692.1998.tb00715.x.

580 Reep, R. L., Stoll, M. L., Marshall, C. D., Homer, B. L. and Samuelson, D. A. (2001) 'Microanatomy  
581 of facial vibrissae in the Florida manatee: the basis for specialized sensory function and  
582 oripulation', *Brain, behavior and evolution*, 58(1), pp. 1-14. doi: 10.1159/000047257

583 Reidenberg, J.S. and Laitman, J.T. (2009). 'Cetacean prenatal development' in Perrin, W.F., Würsig,  
584 B. and Thewissen, J.G.M. (Eds.) *Encyclopedia of Marine Mammals*. 2<sup>nd</sup> Ed. San Diego, CA:  
585 Academic Press. pp. 220–230.

586 Rice, F. L., Mance, A. and Munger, B. L. (1986) 'A comparative light microscopic analysis of the  
587 sensory innervation of the mystacial pad. I. Innervation of vibrissal follicle-sinus  
588 complexe', *Journal of Comparative Neurology*, 252(2), pp. 154-174. doi: 10.1002/cne.902520203.

589 Rice, F. L. (1993) 'Structure, vascularization, and innervation of the mystacial pad of the rat as  
590 revealed by the lectin Griffonia simplicifolia', *Journal of Comparative Neurology*, 337(3), pp. 386-  
591 399. doi: 10.1002/cne.903370304.

592 Sarko, D.K., Reep, R.L., Mazurkiewicz, J.E. and Rice, F.L. (2007) 'Adaptations in the Structure and  
593 Innervation of Follicle-Sinus Complexes to an Aquatic Environment as Seen in the Florida Manatee  
594 (*Trichechus manatus latirostris*)', *Journal of Comparative Neurology*, 504(October 2007), pp. 217–  
595 237. doi: 10.1002/cne.21446.

596 Sarko, D. K., Rice, F. L. and Reep, R. L. (2011) 'Mammalian tactile hair: divergence from a limited  
597 distribution', *Annals of the New York Academy of Sciences*, 1225(1), pp. 90-100. doi:  
598 10.1111/j.1749-6632.2011.05979.x

599 Schröder, H., Moser, N. and Huggenberger S. (2020). *Neuroanatomy of the Mouse*. 1<sup>st</sup> ed. Heidelberg:  
600 Springer.

601 Slijper, E.J. (1962). *Whales*. New York: Basic Books.

602 Trillmich, F. (1981) 'Mutual mother-pup recognition in Galapagos fur seals and sea lions: cues used  
603 and functional significance' *Behaviour*, 78(1-2), pp. 21-42. doi: 10.1163/156853981X00248.

604 Van Horn, R. N. (1970) 'Vibrissae Structure in the Rhesus Monkey' *Folia Primatologica*, 13(4), pp.  
605 241–285. doi:10.1159/000155325.

606 van Kann, E., Cozzi, B., Hof, P. R., and Oelschläger, H. H. (2017) 'Qualitative and quantitative  
607 analysis of primary neocortical areas in selected mammals' *Brain, Behavior and Evolution*, 90(3),  
608 pp. 193-210. doi 10.1159/000477431.

609 Waite, P. M. E. and Ashwell, K. W. S. (2012). 'Chapter 31 - Trigeminal Sensory System' in Mai, J.  
610 K. and Paxinos, G. (Eds.) *The human nervous system*. London: Academic press. pp. 1110-1143.

611 Waite, P. M. E., Marotte, L. R., and Mark, R. F. (1991) 'Development of whisker representation in  
612 the cortex of the tammar wallaby *Macropus eugenii*' *Developmental Brain Research*, 58(1), pp. 35–  
613 41. doi:10.1016/0165-3806(91)90234-a.

614 Woolsey, T. A. and Van der Loos, H. (1970) ‘The structural organization of layer IV in the  
615 somatosensory region (SI) of mouse cerebral cortex: the description of a cortical field composed of  
616 discrete cytoarchitectonic units’, *Brain research*, 17(2), pp. 205-242. doi: 10.1016/0006-  
617 8993(70)90079-x

618 Yablokov, A. V., Bel’kovich, V. M. and Borisov, V. (1974). *Whales and dolphins: Part II*. JPRS  
619 Translation.

620 Yablokov, A. V. and Klevezal, G. A. (1964). ‘Vibrissae of whales and seals, their distribution,  
621 structure and significance’ in Kleynenberg, S.E. (Ed) *Morphological Features of Aquatic Mammals*.  
622 Moscow: The Science Publishing House. pp. 48-81.

623

624 **Tables:**

625 **Table 1:** Origin of specimens

| ID    | Species             | Sex | Age class | Origin                      |
|-------|---------------------|-----|-----------|-----------------------------|
| # 83  | <i>T. truncatus</i> | M   | Newborn   | Died in a marine theme park |
| # 114 | <i>T. truncatus</i> | M   | Newborn   | Died in a marine theme park |
| # 123 | <i>T. truncatus</i> | F   | Newborn   | Died in a marine theme park |
| # 124 | <i>T. truncatus</i> | M   | Newborn   | Died in a marine theme park |
| # 144 | <i>T. truncatus</i> | M   | Newborn   | Died in a marine theme park |
| # 145 | <i>T. truncatus</i> | M   | Newborn   | Died in a marine theme park |
| # 162 | <i>T. truncatus</i> | M   | Newborn   | Wild                        |
| # 229 | <i>T. truncatus</i> | M   | Newborn   | Died in a marine theme park |
| # 146 | <i>T. truncatus</i> | M   | Adult     | Died in a marine theme park |
| # 159 | <i>T. truncatus</i> | M   | Adult     | Died in a marine theme park |
| # 444 | <i>T. truncatus</i> | M   | Adult     | Wild                        |

626

627 **Table 2a:** List of the primary antibodies used for immunoperoxidase (IP) or immunofluorescence  
628 (IF).

| Primary antibody                              | Used for | Immunogen /host   | Supplier  | Dilution | Antibody RRID  | Validation                     |
|---|----------|-------------------|---|----------|----------------|--------------------------------|
| <b>Protein Gene Product 9.5 (PGP 9.5)</b>     | IP       | Polyclonal rabbit | Millipore, Temecula, CA, USA                              | 1:500    | AB_91019       | PMID:19296476                  |
|   | IF       |                   |   | 1:1000   |                |                                |
| <b>Substance P (SP)</b>                       | IP       | Polyclonal rabbit | Immunostar, Hudson, WI, USA                               | 1:1000   | AB_572266      | PMID:10087030<br>PMID:10196365 |
|   | IF       | Monoclonal rat    | Fitzgerald Industries International, North Acton, MA, USA | 1:200    | AB_2313816     | PMID:22740069<br>PMID:26713509 |
| <b>Calcitonin Gene Related Peptide (CGRP)</b> | IP/IF    | Monoclonal mouse  | Santa Cruz Biotechnology Inc., CA, USA                    | 1:200    | AB_2259462     | PMID:30971286<br>PMID:29943954 |
|   | IF       | Polyclonal rabbit | Peninsula Laboratories Inc., San Carlos, CA, USA          | 1:1000   | AB_2313775     | PMID:18186028<br>PMID:28680400 |
| <b>Human Tyrosine Hydroxylase (TH)</b>        | IP/IF    | Monoclonal mouse  | Monosan, Uden, Netherlands                                | 1:50     | ID: MONX10786* | PMID:29615733                  |
| <b>Neurofilament 200kDa (NF 200kDa)</b>       | IP/IF    | Monoclonal rabbit | Sigma, Saint Louis, Missouri, USA                         | 1:1000   | AB_477272      | PMID:18022951<br>PMID:19937712 |

629



630 **Table 2b:** List of the secondary antibodies used for immunoperoxidase (IP) or immunofluorescence  
 631 (IF).

| Secondary antibody              | Used for | Immunogen /host | Supplier                                   | Dilution | Antibody RRID | Validation                     |
|---------------------------------|----------|-----------------|--|----------|---------------|--------------------------------|
| <b>Biotinylated Anti-Rabbit</b> | IP       | Goat            | Vector Laboratories, Burlingame, CA, USA   | 10 µg/ml | AB_2313606    | PMID:19127523<br>PMID:23766132 |
| <b>Anti-Mouse</b>               | IP       | Goat            | Vector Laboratories, Burlingame, CA, USA   | 10 µg/ml | AB_2336171    | PMID:23766132<br>PMID:25057794 |
| <b>Anti-Mouse Alexa 594</b>     | IF       | Goat            | Thermo Fisher Scientific, Waltham, MA, USA | 1:200    | AB_141372     | PMID:23913443<br>PMID:25057190 |
| <b>Anti-Rat Alexa 594</b>       | IF       | Donkey          | Thermo Fisher Scientific, Waltham, MA, USA | 1:200    | AB_2535795    | PMID:25933105<br>PMID:28089909 |
| <b>Anti-Rabbit-FITC</b>         | IF       | Goat            | Calbiochem, Darmstadt, Germany             | 1:100    | ID: 401314*   | PMID:29615733                  |

632 \*Antibody RRID are universally identified codes and were taken from the website the antibody  
 633 registry (<https://antibodyregistry.org/>) which integrated the antibody database of the *Journal of*  
 634 *Comparatve Neurology*. For each antibody, there is at least one publication correlated to a unique  
 635 PMID (PubMed Identifier). For the antibodies whose lot number are MONX10786 and 401314, there  
 636 are still no current RRID available but the validation appears in one publication (Bombardi et al.,  
 637 2010).  
 638

640 **Figure legends**

641

642 **Figure 1** – Rostrum of some specimens of (a) newborn and an (b) adult bottlenose dolphin. The  
643 arrows indicate where the VS emerge from the skin (a) or the concavity (b).

644

645 **Figure 2** – Longitudinal section of a typical FSC in newborn bottlenose dolphin. a. The vibrissa is  
646 surrounded by a venous sinus (s). A capsule (cp) envelops the complex. Several nerves (arrows) reach  
647 the root of the vibrissa. The arrowhead indicates the fusion between the capsule and mesenchymal  
648 sheath. b. Detail at higher magnification of the epidermal components. c. Detail at higher magnification  
649 of the dermal components. b, bulb; cp, capsule; gm, glassy membrane; irs, inner root sheath; ms,  
650 mesenchymal sheath; ors, outer root sheath; p, papilla; s, venous sinus; vs, vibrissal shaft. Masson's  
651 Trichrome stain. Scale bars: a = 1 mm; b, c = 100  $\mu$ m.

652

653 **Figure 3** – Innervation of the FSC in a newborn bottlenose dolphin. The nerve fibers were  
654 immunolabelled for PGP 9.5 (a-d) and NF200kD (e, f). a. Several PGP 9.5-ir nerve bundles (asterisks)  
655 reach the root of the vibrissa. p, papilla. b. Few thin-calibre fibers (arrowhead) enter the papilla (p)  
656 and terminate as free nerve endings (arrows). c. In the mesenchymal sheath, some nerve fibers (arrow)  
657 give rise to MNEs (asterisks). d. High magnification showing MNEs. Note the characteristic button-  
658 like endings. e. The dense network of nerve fibers around the bulb. f. A nerve bundle penetrates the  
659 FSC laterally. vs, vibrissal shaft. Scale bars: a, e = 100  $\mu$ m; b, c, f = 200  $\mu$ m; d = 50  $\mu$ m.

660

661 **Figure 4** – Longitudinal (a) and transverse (b-i) sections (b) of FSC in newborn bottlenose dolphin  
662 showing the innervation at different levels from the basal (b) to the apical (i). The nerve fibers were  
663 immunolabelled with antibodies to PGP 9.5. b. Some nerves (arrows) reach the root of the vibrissa.  
664 c. The nerves break into several fascicles (arrows) that ascend close to the papilla (p). d. The nerve  
665 fibers (arrows) surround the follicle. e. Some nerve fibers (arrows) penetrate the venous sinus (s) and  
666 branch in the mesenchymal sheath (arrowhead). vs, vibrissal shaft. f. Some fibers terminate on MNEs  
667 (arrowhead), while others continue along the FSC (arrow). g. A nerve fiber (arrow) passes through  
668 one of numerous trabeculae of the venous sinus. h. At the level of dermo-epidermal border, the nerve  
669 fibers disappear but the MNEs are still present (arrow). i. Section through the skin and the dermal  
670 papilla. Scale bars: a = 1 mm; b-h = same magnification of i; i = 350  $\mu$ m.

671

672 **Figure 5** – SP- (a, b) and TH-(c-f) immunoreactive fibers in newborn bottlenose dolphin. a.  
673 Transverse section of a nerve bundle showing many immunoreactive fibers. b. A nerve fiber (arrow)

674 runs parallel to a blood vessel (asterisk). c, d. Double immunofluorescence PGP 9.5-FITC (c) / TH-  
675 Alexa 594 (d) of a nerve bundle in transverse section. Note the TH immunoreactivity of some fibres.  
676 e. Several nerve fibers (arrows) reach the tunica adventitia of a vessel (asterisk). f. A thin fiber run  
677 within the MS. Scale bars = 100  $\mu$ m.

678

679 **Figure 6** – Longitudinal sections of FSC in adult bottlenose dophin. The nerve fibers were  
680 immunolabelled for PGP 9.5 (a, b) and NF200kD (c, d). a. Note the six nerve bundles (arrows)  
681 reaching the FSC. b. A vibrissa is clearly visible inside the follicle. Some nerve fibers (arrows) reach  
682 the bulb, others (arrowheads) run within the MS. b, bulb; p, papilla; vs, vibrissal shaft. c. High  
683 magnification showing the rich innervation (arrows) of the MS. d. Detail of a MNE (arrow). Scale  
684 bars: a, b = 1 mm; c = 200  $\mu$ m; d = 100  $\mu$ m.

685

686 **Figure 7** – SP- (a, b) and TH- (c-e) immunoreactive fibers in an adult bottlenose dolphin. a. Two  
687 positive fibers reach the FSC laterally. b. Few nerve fibers in the MS. c, d. Double  
688 immunofluorescence PGP 9.5-FITC (c) / TH-Alexa 594 (d) of a large nerve bundle in longitudinal  
689 section. Note the few TH-ir fibers. e. Few fibers (arrow) in the MS. Scale bars: a, b, e = 200  $\mu$ m; c, d  
690 = 100  $\mu$ m.

691

692 **Figure 8** – Schematic drawn representing the main differences between the FSCs of a terrestrial  
693 mammal (left), pinniped (center) and dolphin (right). On the right, the follicle represented is that of  
694 the adult as the dotted lines and transparent areas (SVNs and MNEs in the dermo-epidermal junction)  
695 are of the newborn. In terrestrial mammals the FSC is divided into two halves, the inferior cavernous  
696 sinus, and the superior ring sinus. The receptors are of various nature, are positioned at various heights  
697 depending on their receptor (sensory) nature and come mainly from the deep vibrissal nerve. In the  
698 pinniped it is instead divided into three portions, including an upper cavernous sinus. In this case,  
699 however, the fibers, which derive only from the deep vibrissal nerve, innervate up to the inner conical  
700 body, without reaching the epidermis. Finally, in the dolphin there is a trabecular component that  
701 forms a single venous sinus in which the receptors, deriving mainly from the deep vibrissal nerve, are  
702 distributed along the follicle until they reach the epidermis in the newborn. Also note the TH-ir  
703 (green) and SP-ir (light blue) fibers which accompany the blood vessels. Abbreviations: VS, vibrissal  
704 shaft; e, epidermis; irs, inner root sheat; ors, outern root sheat; ms, mesenchymal sheat; ocb, outern  
705 conical body; icb, inner conical body; rw, ringwulst; rs, ring sinus; cs, cavernous sinus; lcs, lower  
706 cavernous sinus; ucs, upper cavernous sinus; c, capsule; p, papilla; b, bulb; DVN, deep vibrissal  
707 nerve; SVNs, superficial vibrissal nerves; MNEs, merckell nerve endings; FNEs, free nerve endings;

708 CEs, circular endings; LEs, lanceolate endings; REs, reticular endings; a, artery; v, vein; vs, venous  
709 sinus.

710

711 ~~Figure 9~~ Schematic representation of the course of the maxillary nerve (V2) in adult (left) and  
712 newborn (right) bottlenose dolphin. The dotted ellipse approximates the area of the FSCs location.

713